How temporal turnover in community composition is linked to anthropogenic pressure.

J. Christopher D. Terry (1,2) christopher.terry@biology.ox.ac.uk (Corresponding Author) 0000-0002-0626-9938

Axel G. Rossberg (1) a.rossberg@qmul.ac.uk 0000-0001-9014-3176

1: School of Biological and Behavioural Sciences, Queen Mary University of London, London, UK

2: Department of Biology, University of Oxford, Oxford, UK.

Abstract

Understanding the mechanisms behind biodiversity change through time is central to assessing and forecasting anthropogenic impacts on ecological communities. While some local temporal turnover in species composition is natural and indeed underpins ecosystem resilience, it may also indicate external pressure on an ecosystem. Here, we assess how human impacts (via the Human Modification Index synthetic proxy) affect multiple metrics of bird community composition turnover across 2692 transects of the North American Breeding Birds Survey from 27 Bird Conservation Regions over 50 years. Against a background of constant species richness, we find total anthropogenic impact to be consistently associated with greater turnover at long-timescales (reduced asymptotic similarity), but a slightly slower rate of short-term turnover (initial similarity decline). A third turnover measure, the exponent of species accumulation through time, was not notably influenced by humans. Taken together, these results give a new window into ecological community dynamics. In particular, we can identify that intrinsically-driven species turnover is slowed by humans, but turnover determined by extrinsic changes to the ecosystem increases. More widely, our analysis suggests a greater role for intrinsic dynamics in interpreting observed temporal beta-diversity and that anthropogenic impact assessments based on short-term rates of change may be incomplete.

Introduction

Change through time is the only true constant within ecological communities. Understanding these changes is central to both core theories of biodiversity[1–3] and applied efforts to link biodiversity change to anthropogenic pressures[4]. Behind relatively stable tallies of species richness (α-diversity) there is often considerable turnover in species composition (temporal β-diversity)[5], which appears to be considerably faster than would be expected by neutral models[6]. However, quantifying and summarising these changes remains a challenge as β-diversity is a fundamentally multi-facetted concept[7] and it is increasingly established that species richness trends are not necessarily correlated with wider biodiversity trends[8,9].

Despite its acknowledged importance, temporal β-diversity has received less attention than spatial patterns, at least in part due to the challenges in gathering sufficient data[10]. Meta-analyses of observations of year-on-year turnover rates have identified latitudinal gradients[11], higher rates of change in marine systems[12], identified a link between temperature changes and turnover rates in marine systems[13], and interactions between 'naturalness' and the rate of climate change[14]. However, fundamental questions remain to be comprehensively addressed, in particular the extent to which species turnover through time at a particular location is determined by external changes to the ecosystem or represents dynamics intrinsic to a given system[15].

The two aspects of temporal β-diversity most frequently studied to date have been: 1) the slopes of species accumulation curves (also termed the species-time relationship, STR[16,17]) and 2) measures of the rates of species gains and losses[12–14]. The second can either be directly reported or captured by similarity measures such as the Sørensen or Jaccard indices, which can then be partitioned to account for changing species richness[18,19]. Both aspects have been referred to as 'turnover', although they capture distinct ecological patterns. In particular, the STR captures the rate of appearance of 'new' species, while composition similarity measures could indicate high turnover from the same species repeatedly colonising and being extirpated. The exponent of the STR is affected by the dynamics of rare or ephemeral species, but does not capture information about the permanence or otherwise of core species.

Nevertheless, any single rate of 'turnover' is inevitably an average over the community, obscuring the inter-specific differences in residence time, extinction and recolonisation probability[20] and differentiation between 'core' and 'occasional' species[21]. Unless there are strong cyclic dynamics[22], the similarity of communities will decline through time. However, across 'ecological' time scales in non-successional systems we would expect the decline in similarity to asymptote at a value considerably above zero[23]. Determining this asymptote requires long time series, but could be highly

informative about the nature of the underlying ecological dynamics. In particular, in contrast to short-term turnover, it describes the 'depth' of the turnover and is influenced by the proportion of species that can be considered 'core' species.

Here we take a multiview perspective of turnover to examine the fundamental drivers of ecological change in a uniquely large and methodologically consistent dataset, the North American Breeding Bird Survey (BBS[24]). Specifically, we test two propositions: (1) if human impacts on turnover are detectable, and (2) whether they are consistent across turnover metrics. We quantify a suite of aspects of species turnover (Fig 1) for 2692 transect routes from 27 Bird Conservation Regions (BCRs, Fig 2) that met our criteria for inclusion and fit a series of hierarchical regression models using as predictors key putative drivers of turnover. We represent total anthropogenic impacts on each transect using a synthetic proxy, the highly spatially resolved Human Modification Index[25]. This incorporates thirteen anthropogenic stressors including population density, land use and transport infrastructure. We also include in our statistical models the average observed species richness on the transect, the size of the wider species pool (derived from intersecting transect routes with highly resolved range maps[26]), a measure of interannual environmental variability (based on the coefficient of variation in gross primary productivity, derived from MODIS satellite data), and the duration of available data as a further methodological control variable. Focussing on bird species that are well captured by the survey methods, we determined for each BCR the influence of key drivers on species richness trends (Fig 1b), the exponent of the species accumulation curve (Fig 1c), and four aspects of the shape of Sørensen's similarity decay curves (Fig 1d). We then conduct a meta-analysis across the Bird Conservation Regions to identify any overall effect.

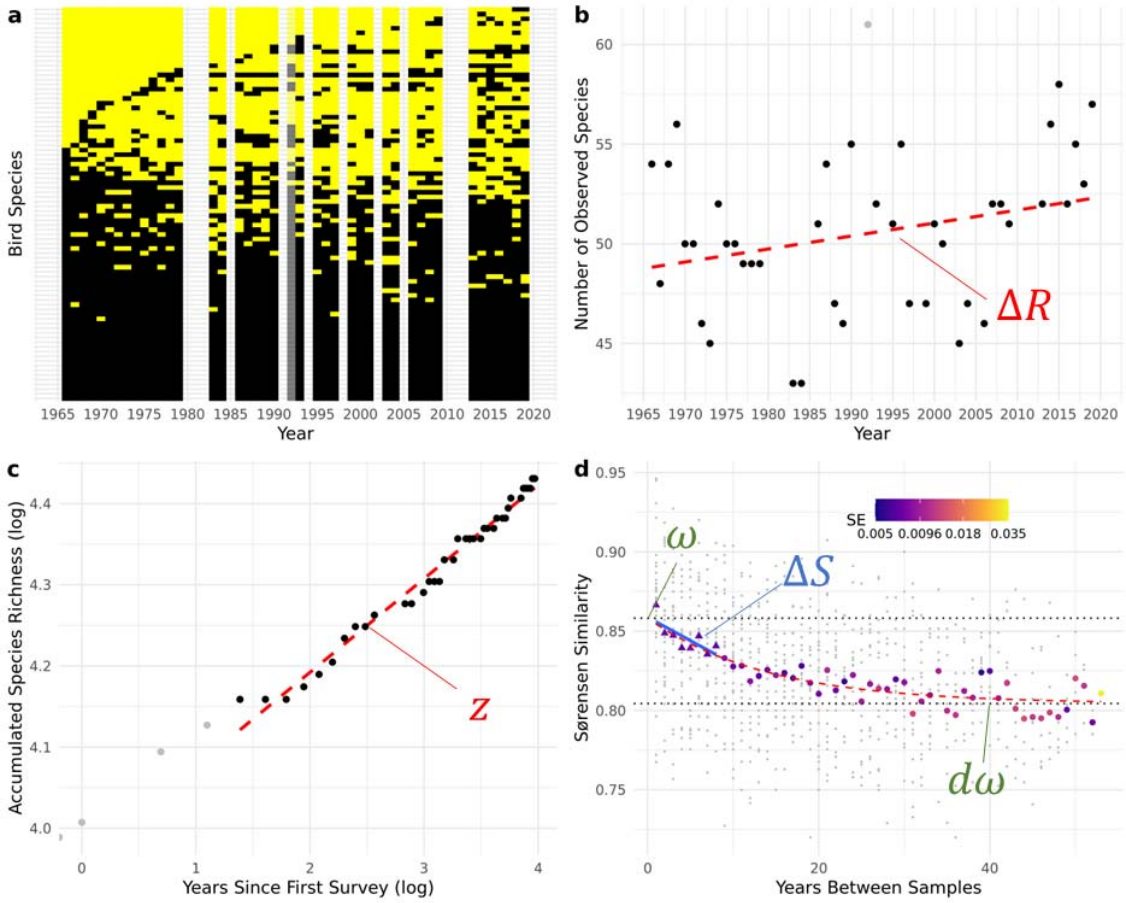

Fig. 1 Example transect data illustrating the form of the data and the derived statistics. The example here is the 'Pine Grove' transect (C_840_S_02_R_008), located in the 'Appalachian Mountains' Bird Conservation Region (Lat: 34.0, Long: -85.7). a) *Species presence-absence matrix*. Only years where there was a survey that passed the BBS quality control are included. Black filled tiles indicate species presence. Species are ordered by the year they are first seen. Data for 1992 is shown in grey – it was excluded from further calculation as the number of species observed was larger than 2 SE of the mean. b) *Observed species richness trend.* Linear model summarising trend is shown with dashed line (slope = +0.0651 sp year^{-1}). Excluded year (1992) is shown in grey. c) *Rate of species accumulation* (species-time relationship). Here the total number of species observed at least once since the start of the survey is regressed against time since the first survey. A linear model is fit on a log-log scale, excluding the first 4 points (shown in grey). Here, the slope (exponent) was 0.115. d) *Community similarity decay curve.* Small grey dots show raw Sørensen similarities of each year-pair. Coloured shapes show mean similarity values for each year-difference, with the colour indicating the standard error of the mean used in the model fitting. Fitted initial rate of similarity decay ( ) for the first 8 points (triangles) is shown with a solid blue line. Note that in order to make a more positive value correspond to a faster turnover, the sign of the slope is reversed to calculate The similarity decay curve fit (red dashed line) follows , where here d: 0.937, : 0.858, L: 0.0715. Black dotted lines show fitted maximum observed similarity at t=0, ( ), and asymptotic observed similarity ( ).

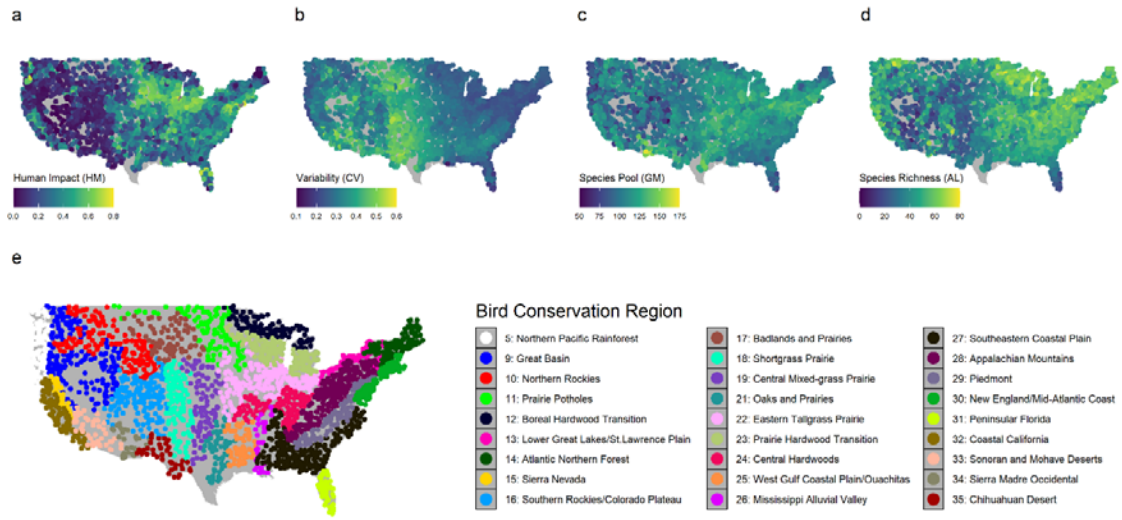

Fig 2. Distribution of the values for four predictor variables for each transect across the United States and allocation of the transects to Bird Conservation Regions (BCRs) of the focal transects. a) Human impact proxy, derived from the Human Modification Index map, b) an environmental variability proxy derived from the coefficient of variation of satellite derived Gross Primary Productivity, c) the size of the species pool, derived from eBird range map data, and d) average observed species richness from the transect surveys. The fifth predictor variable used, the year span of surveys available for each transect is not shown here as it shows no meaningful spatial pattern. Points are visualised at the start of each 40 km route. While predictor variables are strongly correlated at the continental scale, within BCRs the correlations are markedly weaker (SI1). e) the location and brief description of each Bird Conservation Region that were each initially fit as separate analyses.

Results

The shape of the similarity decay curve could be well described by our bounded exponential decay model:

$$\overline{S_{t,i}} \sim \omega_i[(1-d_i)e^{-L_i t} + d_i]$$

where $\overline{S_{t,i}}$ is the mean Sørensen's similarity between transects separated by t years in transect i. See SI 4 for examples. The model had three control parameters, ω (observation accuracy), L (similarity decay rate) and d (asymptotic community similarity). Across the 27 focal Bird Conservation Regions (BCRs), there was remarkable consistency in the impact (or lack of impact) of our putative determinants of the similarity decay curve (SI 2).

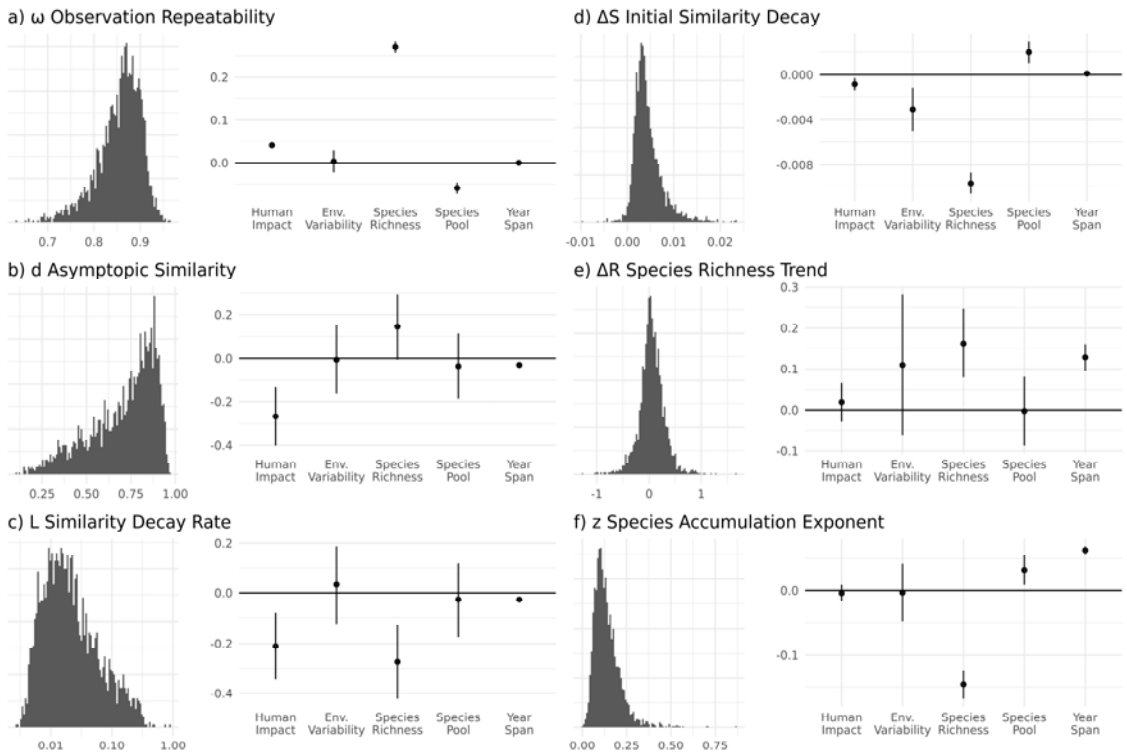

Fig.3. Histograms of fitted turnover statistics across all transects and estimated effects of the key predictor variables across all Bird Conservation Regions (BCRs). The overall impact of the predictors shown on each right column is effectively a meta-analysis of the coefficients identified in each of the 27 focal BCRs. Separate BCR-level results are shown in SI 2. Predictor variables are each scaled to approximately 0-1 range prior to centring (Year Span /50, Species richness /100, Species pool /150), but the magnitude of impact should not be considered directly comparable between predictors. Lines show central 90% of posterior distribution.

The total distribution of fitted response parameters and impact of predictor variables across all regions are shown in Fig 3. Overall, higher human modification was associated with greater observation accuracy (ω, Fig 3a), lower asymptotic similarity (d, Fig 3b) and slower rate of similarity decay (L, Fig 3c). Higher average observed species richness were associated with significantly greater ω, lower L and greater d. Larger regional species pools were associated with marginally lower ω, but no clear impact on d or L. Environmental stochasticity, as described by productivity variability, was not consistently influential and study duration had negligible impact on the parameters of the similarity decay curve. In our model an L value of approximately 0.028 would correspond to a 'half life' of similarity decay of 25 years, implying that a considerable proportion of the transects show a levelling off in the decline of similarity on the timescales of the dataset.

The initial rate of similarity decay (ΔS), as measured by a direct linear model through the early stages of the similarity decay curve, was slightly reduced by human modification – i.e. higher levels of anthropogenic impact were associated with slower short-term turnover. However, initial rates of

decay were much more influenced by the observed species richness (higher average observed species richness was strongly associated with slower initial decline in similarity) and the impacts were comparatively inconsistent across BCRs (SI 2).

Observed species richness was remarkably consistent through time on most transects (Fig 3e), in line with previous results with this dataset[27], although see[28]. Across all transects, the mean change in richness was low: +0.053 species per year, equivalent to around two additional species between the start and the end of the survey period. With an average of 45.7 species seen on each transect, this is a small proportional change. This near-balance between gains and losses justifies our focus on a simple measure of community similarity rather than seeking to partition out the dissimilarity due to changing species richness. Our suite of predictors could not consistently explain a notable portion of the variation in species richness trends (mean adjusted-R^2 across all BCRs = 0.046). Transects with higher observed richness or greater spans of available data showed more positive trends.

The accumulation of observed species after t years (sp_t) could be well described by a standard STR function: $\log(sp_t) \sim \mathrm{z}\log(t) + \mathrm{c}$ where the overall mean species accumulation exponent (z) across all transects was 0.156 (Fig 3f). Average observed species richness was consistently negatively correlated with this exponent, in line with previous analyses[16]. Transects with a longer duration of data had marginally higher exponents. The Human Modification Index had no detectable impact, while other relationships with the predictor suite were small in relative magnitude and inconsistent between BCRs (SI 2).

Discussion

We found consistent and pervasive human impacts on species turnover between the bird communities across habitats, but crucially these effects depended on the aspect of 'turnover' considered. Taken together they give a deeper picture of the fundamental ecological dynamics with significant implications for the interpretation of short-scale monitoring programs for conservation objectives.

Our proxy for anthropogenic disruption, the Human Modification Index[25], was consistently associated with lower asymptotic similarity (d). By contrast, the exponent of the species-accumulation curves (z) was not clearly related to the Human Modification Index, once differences in average species richness had been accounted for. Furthermore, the initial short-term rate of similarity decline (ΔS), a frequently examined method of assessing turnover, showed marginally *slower* turnover in areas of higher human modification. Hence, core measures of 'turnover' appear to give contrasting inferences of anthropogenic impact.

These differences have clear implications for the use of single measures of observed turnover for conservation objectives – inferences of one aspect of turnover may not translate to others. A frequent objective of turnover studies has been to determine a single annualised rate of species extinction and colonisation[29]. Multiple authors have sought to identify ideal sampling frequencies and analyses to better capture this quantity[22,30–32], traversing the twin perceived threats of missing species extirpation and recolonisation between censuses (crypto-turnover) and of failing to consistently observe present species (pseudo-turnover). Our results suggest that this may risk obscuring important dynamics and suggests that arguments identifying higher short-term turnover as an indicator of anthropogenic impact (and hence conservation focus[12]) may need to be reassessed.

The divergences also offer the opportunity to triangulate the relative role of intrinsic and extrinsic processes in determining how anthropogenic effects translate into biodiversity changes (Fig. 4). The similarity of a community as recorded between two timepoints is determined by a multitude of processes. Leaving sampling effects to one side, fundamentally these can be categorised into intrinsic and extrinsic drivers (Fig 4). Intrinsic turnover incorporates the processes that would generate ongoing turnover without long-term external change. This includes the impact of demographic stochasticity, dynamics generated by interspecific interactions between species within the existing metacommunity[15] and any local species turnover driven by 'background' environmental stochasticity[33]. By contrast, extrinsic drivers change the foundations of the community, and include long term climate and land-use changes and shifts to the species pool in the wider metacommunity (whether through range shifts or longer term processes such as speciation).

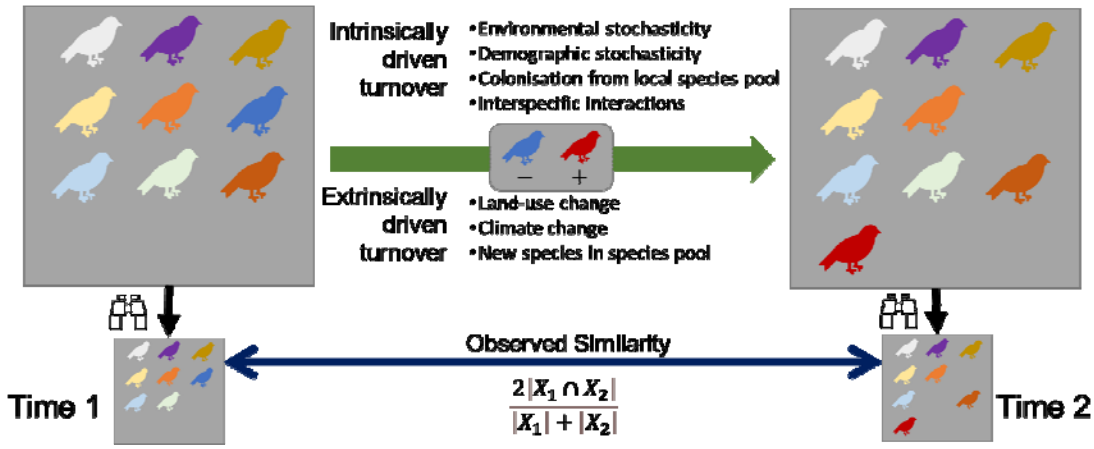

Fig 4. Contributing factors to the observed similarity of ecological communities between two time points. Changes in the occupancy of a site can be affected by multiple intrinsic and extrinsic drivers, making disentangling the underlying drivers a significant challenge. Here, the blue bird is lost and the dark red bird is gained between the observation points. The observed similarity will be deflated due to observation errors (principally false-absences).

Identifying the extent of intrinsic turnover is crucial to understanding whether observed changes in species composition are a concern or in fact an indication of a healthy resilient ecosystem undergoing 'normal' dynamics[4]. It is also important to understand whether changes in the rate of observed turnover between communities are directly due to external drivers or due to modification to the intrinsic dynamics of the system. The observation of a clear levelling off in similarity in many transects suggests that intrinsic turnover dominates the observed turnover dynamics, since sustained and directional extrinsically driven turnover would be expected to drive continually declining similarity. Previous work with island bird communities[23] suggested that the timescales at which these processes were dominant were sufficiently different that they could be differentiated. However, given the rate at which global change is progressing, this assumption is unsafe. Extrinsic changes may plausibly be occurring on similar 'intermediate' time scales to intrinsic turnover and extensive previous work on North American birds has demonstrated that some bird species' range and abundance changes are attributable to extrinsic drivers[34,35]. Nonetheless, it is still reasonable to assume that the relative balance between extrinsic and intrinsic factors is tilted more towards intrinsic processes at shorter time scales.

The rate of species accumulation in over sequential samples, often referred to as the species-time relationship ('STR'[36]), provides an additional route to qualitatively differentiate the impact of humans on intrinsic and extrinsic processes. Since extrinsic changes can be expected to result in the arrival of 'new' species at a faster rate compared to intrinsic turnover, increases in extrinsically driven turnover would be expected to increase the exponent . The minimal impact of humans on

219 the rate of species accumulation suggests that, for this turnover measure at least, any human-driven
220 increases in the arrival of novel species are being matched by a reduction in the background rate of
221 turnover. Extrinsic changes in the environment due to human modification are impacting long-term
222 turnover through shifts in the status of species from 'rarely seen' to 'frequently seen' (and vice-
223 versa) rather than simply an increased rate of appearance of 'new' species.

224 To summarise, at the transect scale of our study human impacts are generally causing a slower, but
225 deeper, mixing of the species pool that is largely already present in the wider metacommunity.
226 Intrinsic dynamics appear to have a key role in determining observed turnover, upon which are
227 overlaid the impacts of extrinsic drivers of turnover, such as land use change[35,37]. Concordant results
228 were also found in long term surveys of Canadian trees[38] where, although community wide
229 functional trait shifts driven could be detected, the role of ongoing disturbances had a greater
230 impact on turnover than environmental change.

231 A moderate slowdown of short-term turnover due to human impacts may appear counter-intuitive,
232 particularly as known reductions in the population abundance of many species[27,34] may erode the
233 sustainability of local species populations. However, there are several possible explanatory
234 mechanisms for this effect. Any possible impact pathways need to be considered in the light of the
235 observation of only slight trends in species richness across the study period[27]. This implies that
236 overall extirpation and colonisation on the transects are approximately balanced. Most directly,
237 observed slow-downs of turnover with human impact could be a manifestation of a shifting baseline
238 – if more highly impacted areas had already lost many rare and ephemeral species before the start
239 of the survey period, this could explain the reduction in short-term turnover. This hypothesis is hard
240 to directly test without older baseline data, however, we note that there was minimal correlation
241 between observed species richness and our human modification proxy (within BCR average
242 Pearson's correlation = -0.0006, SI 1bii).

243 Human modification could also be associated with slower turnover directly, by reducing the causes
244 of intrinsic turnover, in particular by slowing colonisation rates or weakening interspecific
245 interactions. However, precisely diagnosing specific mechanisms from observation data such as this
246 is a considerable challenge. The effective balance in species richness could be attributable to
247 extinctions contributing to opening up niches for new colonists to fill, or colonisation may lead to
248 exclusion of previous residents from the community. Directly distinguishing gap exploitation from
249 displacement driven turnover is not straightforward from observational data, particularly as
250 individual cases of extirpation and colonisation can lead to either homogenisation or
251 heterogenization between two samples[39]. In a scenario corresponding to a saturated (structurally

252 unstable[40]) community, if human impacts led to a reduction in the rate of colonisation of sites along
253 the transect from the wider metacommunity the short term rate of turnover would fall.

254 At the scale of presence/absence on BBS transects we are unaware of direct evidence for
255 widespread competitive exclusion between species, although there are examples of competitive
256 exclusion in birds in other systems[41,42]. However, given the complexity of possible interactions, we
257 would not necessarily expect clearly observable patterns of exclusion to result from competition[43,44].
258 Turnover driven by continual immigration events has been shown to be able to reproduce a host of
259 observed patterns in models where the total diversity of a community is in some way limited[45], such
260 that each colonisation tends to lead on average to an extinction from the community. Colonisation
261 pressure is likely to be positively linked to the diversity of the species pool (i.e. gamma diversity) and
262 we do see small positive associations between the species pool and both the initial similarity decline
263 and species accumulation exponent. Further research into the underlying mechanisms behind
264 intrinsic turnover will be highly valuable. Analysis of trends in functional diversity[28] may be able to
265 identify signals of trait-based species sorting.

266 The four ecological predictors that we built into our regression models each capture a variety of
267 processes and need to be interpreted with care. Human impacts have not been consistent through
268 time, and the state of modification at the end of the time period (the Human Modification Index is
269 based on data with a median year of 2016), will obscure differences between areas where there was
270 large scale land-conversion during the last 50 years, and those where human impacts were already
271 at a high level long before the surveys started. Further, the BBS survey was not initially designed in a
272 fully structured way, and as such there are potentially problematic links between survey period and
273 ecological predictors. For example, earlier-starting transects with longer data spans tend to be in
274 relatively more human-modified areas, while recent heavy land use change has been found to be
275 associated with the early stopping of transect data collection[46]. As a quantitative assessment of the
276 total extent of changes to turnover across the US may be beyond reach we therefore focus on
277 identifying the direction of links between our predictors and biodiversity responses.

278 While all the transects cover the same distance and use the same protocol, there are significant
279 differences in their route shape and the heterogeneity of the habitat that they cross. This
280 heterogeneity is known to influence observed species richness[47]. Our measure of average observed
281 species richness is therefore unlikely to represent only the classic understanding of alpha diversity as
282 being the number of species existing in a particular point location. A significant habitat
283 heterogeneity component could provide a mechanistic explanation of why the initial rate of
284 similarity decay is slower with higher observed species richness: increased habitat heterogeneity

could reduce the number of potential colonists in neighbouring areas able to drive intrinsic turnover[15]. Similarly, our metric of the size of the species pool (the number of bird species ranges the transect route crosses), will also be affected by the heterogeneity of habitat crossed by the route. This may explain the negative relationship between species pool and observation error. A route that crosses a greater variety of habitat subtypes will inevitably have less observation time in each, and a higher likelihood of missing specialists. Although the range maps are fundamentally porous and are so likely to overestimate the real species pool at any given location[48], it is reasonable to expect a good correlation.

Our intercept term, ω, is designed to account for the apparent dissimilarity in repeat samples attributable to undetected resident species or the observation of vagrant species passing through, but not truly resident. Our framework assumes that detectability was approximately constant through time. The nearly constant observed species richness suggests this assumption is reasonable. With perfect surveys, similarity at t=0 should be 1. With the bulk of ω values falling between 0.8 and 0.9, missed species contribute notably to apparent turnover between surveys. Previous studies that have directly assessed measurement error using raw stop-level count data have identified strong differences between transects in average detectability of species[49,50]. It is likely that differences in detectability between transects are behind the strong positive association between observed species richness and ω. Our metric of human impact was also associated with increased ω. This could be a measurement effect, such as greater habitat openness and hence fundamental detectability, or a biological effect, where humans cause extirpation of rare, hard to detect species (and consequently raising the average detectability of the remainder).

Conclusion

By taking a holistic view of different aspects of species turnover[10], we have been able to identify a pervasive anthropogenic impact on ecological community dynamics. Highly human impacted regions may not be showing notable changes in species richness, and in fact show somewhat slower rates of short-term community turnover, but they do show deeper long-term community change through time as the community undergoes fundamental changes in structure. This effect appears to be largely driven by changes in the patterns of temporal occupancy within the bird community, rather than the arrival of 'new' species. That said, the recent past is not necessarily a guide to the future, and rates of extrinsic change (particularly climate impacts) are likely to accelerate in the coming decades[51,52]. By focussing on a single taxonomic group with largely consistent sampling protocols, we have been able to undertake a more detailed analysis, but results from meta-analyses with broader scope[13,14] suggest that we should expect considerable differences between taxa and biomes. Our

results highlight the pressing need to understand mechanistically the turnover in ecological communities in order to better interpret future changes.

Methods

Unless otherwise noted, all analyses were carried out in R version 4.2.0. All data used is publicly available.

Bird Data

We collated yearly presence-absence matrices for 2692 transects from the North American Breeding Bird Survey (BBS), using the 2020 release covering data from 1966 -2019[24]. BBS data are collected annually on one day during the peak of the avian breeding season along thousands of survey routes across North America. Surveys follow a standardised protocol allowing comparison of diversity patterns through time[53]. Each route is 40 km long with 50 observation points at approximately 800 m intervals. At each point, observers carry out a 3-min point count during which every bird observed or heard within ~400 m radius is recorded. Raw data is then checked and collated centrally.

We excluded species that were not identified to species level or are poorly captured by the BBS surveying methodology (i.e. nocturnal, crepuscular, birds of prey, and aquatic species) following others[28,54]. Where taxonomic revisions had split or lumped taxa during the survey, these were grouped together as a single taxa for consistency. In most cases these are allopatric divisions and so are unlikely to impact recorded dynamics on individual transects.

We retained data for transects that had associated GPS data for the route (the U.S. Geological Survey Patuxent Wildlife Research Center, http://purl.stanford.edu/vy474dv5024), had more than 11 surveys (in order to generate more than 10 similarity values), and were part of a Bird Conservation Region (BCR[55]) that had at least 25 suitable transects. We excluded all surveys that did not pass the BBS quality control (e.g. the weather was poor). To further reduce the impact of unusual weather or poor surveying, if a particular survey had a reported species richness that deviated from the mean richness by more than twice the standard deviation of richness's for that transect, that survey was excluded (see example in Fig 1, this step excluded 3274 out of 85460 surveys (3.83%)). Our final dataset comprised data from 2692 transects from 27 BCRs, comprised an average of 31.7 (SD = 11.2) surveys, spanning an average of 39.4 years (SD = 11.5). See SI 1 for further summary statistics.

By studying changes in presence-absence rather than abundance[56,57], our study directs focus towards the dynamics of rarer species. Abundance-based analyses frequently find that trends are

dominated by a handful of species[20,58], including with this dataset[35]. In all transects there is a large group of apparently permanent species that are observed in each year in the transect (SI Fig1.A.g).

Predictor Data

We assembled three key predictors variables from cross-referencing the transect GPS routes with external data sources: a measure of the avian gamma diversity (GM), a proxy of inter-annual environmental variability (CV) and a proxy for human impact (HM).

For our gamma diversity predictor (the size of the species pool), we downloaded summer predicted range maps derived from eBird data (the November 2021 release[26,59]). These use large-scale citizen science data and finely resolved environmental predictors to generate high-resolution range maps. We used the spatially smoothed ('medium resolution', 8.89 km^2) maps of all species with range map data that were also included in our BBS transects data (375 species). For each transect, we calculated the total number of species ranges that the transect route intersected. Hence, GM is partly a measure of the heterogeneity of habitats the route crosses.

For inter-annual variability, we used high-resolution MODIS satellite derived Gross Primary Productivity (GPP) data (MOD17A2H V6) accessed through Google Earth Engine (https://developers.google.com/earth-engine/datasets/catalog/MODIS_006_MOD17A2H). For a 1km buffer around each transect route, we calculated the mean GPP for each year from 2001 to 2021 (the period for which complete and consistent data was available). We then calculated the coefficient of variation of annual productivity for each transect. To reduce the effect of a certain high-outliers, we square-root transformed the coefficient of variation to generate our variability proxy 'CV'.

For human impact, we used a global human modification raster map at 1km scale[25], which combines 13 anthropogenic stressors (including population density, agricultural land use, fragmentation and night-time lights) into a single 0-1 'Human Modification Index'. We intersected the transect routes with this map, and took a mean value along the route.

We also calculated an 'observed alpha diversity' predictor (AL), as the mean species richness recorded on the transect. Lastly, the duration of data available (difference in years between the first and last survey at a transect) was included as a year span (YS) moderating variable. For the fitting process and to aid comparison, AL, GM and YS were scaled to approximately the 0-1 range by dividing by 100, 150 and 50 respectively.

Similarity-decay

For each pair of years within each transect, we calculated the Sørensen similarity $\frac{2|X \cap Y|}{|X|+|Y|}$ where X and Y are the set of species observed at each sample. Sørensen's similarity has high capacity to detect change[60]. However, the preponderance of short-time interval data compared to long-interval data poses a challenge for identifying the statistical confidence in trends at long and short intervals simultaneously[22,23]. For each transect (i) and time difference (t), we calculated a mean average similarity $\overline{S_{t,i}}$ and its standard error to propagate forward into the later stages. Where a particular time difference had only a single representative (making direct calculation of standard error impossible) it was assigned the mean standard error for that transect.

The effective multiple re-use and temporal non-independence of observations from each transect poses a fundamental problem of pseudoreplication. In particular, estimating the value of the average similarity of samples separated by a particular number of years, contributes in a complex way to the overall uncertainty. Because each year of observation potentially contributes to multiple year-pairs, and each year-pair contributing to each estimate of $\overline{S_{t_i}}$ is not independent of each other, our primary method somewhat underestimates the uncertainty with which the core curve parameters can be estimated.

To calculate the initial rate of similarity decline (ΔS) for each transect, we fit a weighted linear model through the $\overline{S_{t,i}}$ values, up to t = 8 years (Fig 1d). We then use the negative of the slope as a simple measure of turnover, so that higher ΔS is a faster decline.

Similarity Decay Curve Model Fitting

We fit our model for the decline in similarity values through time with a Bayesian hierarchical model for each BCR separately using the Hamiltonian Monte Carlo sampler STAN[61] accessed through the *brms* (version 2.18.0[62]) interface in R. Response variable uncertainty in each $\overline{S_{t_i}}$ estimate was incorporated by the estimated standard error of the point as calculated above. The core model for each transect was:

$$\overline{S_{t,i}} \sim \omega_i[(1-d_i)e^{-L_i t} + d_i]$$

where:

$$\text{logit}(d_i) = d_0 + \beta^d_{HM} C_{HM_i} + \beta^d_{CV} C_{CV_i} + \beta^d_{AL} C_{AL_i} + \beta^d_{GM} C_{GM_i} + \beta^d_{YS} C_{YS_i} + \epsilon^d_i$$

$$log(L_i) = L_0 + \beta^L_{HM} C_{HM_i} + \beta^L_{CV} C_{CV_i} + \beta^L_{AL} C_{AL_i} + \beta^L_{GM} C_{GM_i} + \beta^L_{YS} C_{YS_i} + \epsilon^L_i$$

and

$$\omega_i = \omega_0 + \beta^{\omega}_{HM} C_{HM_i} + \beta^{\omega}_{CV} C_{CV_i} + \beta^{\omega}_{AL} C_{AL_i} + \beta^{\omega}_{GM} C_{GM_i} + \beta^{\omega}_{YS} C_{YS_i} + \epsilon^{\omega}_i$$

The transect level hierarchical terms ϵ^d_i , ϵ^L_i and ϵ^{ω}_i are considered to be drawn from Gaussian distributions with fitted standard deviations. Here β terms represent coefficients and C terms the centred vectors of predictor data. The residual error term (σ) is also allowed to vary between transects, again following a Gaussian distribution. Priors were chosen to be relatively weak with the aim to aid convergence, but not impact the final result. See SI 6 for full model details and for details of the priors assumed. For each BCR, predictors were first centred by subtracting the mean for that BCR. For each model four chains each of total length 10'000 were run, discarding the first 5000 as burn-in. Key convergence statistics indicated convergence was achieved. Raw STAN code and model fits are available in the online repository. Separately, to estimate the best fit values of the curve parameters we repeated the fitting process but without the regression terms. All other aspects were held the same.

Species Richness Trends and Species Accumulation Rates

We identified trends (ΔR) in the species richness by fitting a linear model of species richness against year for each transect (Fig 1b, observed richness were all well above zero justifying this direct approach). We determined the slope of the species accumulation curve (species-time relationship, STR) for each transect, by fitting linear models of $log(sp) \sim z\ log(t) + c$ (Fig 1c). We used collector's curves from the first year (i.e. a nested design[63]). To minimise the dominant influence of observation error on the initial rate of species accumulation[36], we excluded the first four samples from the slope fitting. In line with other results[2], these z values were highly correlated with exponents derived from the alternative model form $sp \sim z\ log(t) + c$. Then, within each BCR and we tested if each response ($\Delta R, z$), could be predicted by our suite of five predictors using linear regression models.

Cross-BCR 'meta-analysis'

Finally, for each of the six responses (ΔS , $\Delta R, z, \omega, d, L$) we conducted a simple meta-analysis across all BCRs to identify if a consistent effect of each predictor can be identified, where each BCR included in our study was treated as a separate 'study'. For this we used a linear model in *brms* to estimate the mean effect of each predictor, weighting by the standard error of the estimate from the within-BCR model fits.

Acknowledgements

We gratefully acknowledge and thank the thousands of BBS survey participants who annually perform and coordinate the survey. This research utilised Queen Mary's Apocrita HPC facility, supported by QMUL Research-IT. http://doi.org/10.5281/zenodo.438045 . We thank Anne

Magurran, Simon Mills, Tom Brewer, Jacob O'Sullivan and Emmanuel Nwankwo for their comments on manuscript drafts. This work was funded by NERC grant NE/T003510/1 'Mechanisms and prediction of large-scale ecological responses to environmental change'.

Author Contributions

JCDT conceptualised, designed and conducted the research and wrote the manuscript. AGR contributed to the analysis design and interpretation of results. Both authors contributed to manuscript editing.

Code and Data Availability Note

All primary data used is publicly available, as cited in the manuscript. R notebooks covering all analysis steps are available as SI. Please contact the corresponding author for the full datasets.

References

1. MacArthur, R. & Wilson, E. O. *The Theory of Island Biogeography*. (Princeton University Press, 1967).
2. Rosenzweig, M. L. *Species Diversity in Space and Time*. (Cambridge University Press, 1995). doi:10.1017/CBO9780511623387.
3. Hubbell, S. P. *The Unified Neutral Theory of Biodiversity and Biogeography*. (Princeton University Press, 2001).
4. Magurran, A. E. How ecosystems change. *Science* **351**, 448–449 (2016).
5. Dornelas, M. *et al.* Assemblage time series reveal biodiversity change but not systematic loss. *Science* **344**, 296–299 (2014).
6. Gotelli, N. J. *et al.* Community-level regulation of temporal trends in biodiversity. *Sci. Adv.* **3**, (2017).
7. Anderson, M. J. *et al.* Navigating the multiple meanings of β diversity: a roadmap for the practicing ecologist. *Ecol. Lett.* **14**, 19–28 (2011).
8. Hillebrand, H. *et al.* Biodiversity change is uncoupled from species richness trends: Consequences for conservation and monitoring. *J. Appl. Ecol.* **55**, 169–184 (2018).
9. Magurran, A. E. *et al.* Divergent biodiversity change within ecosystems. *Proc. Natl. Acad. Sci. U. S. A.* **115**, 1843–1847 (2018).
10. Magurran, A. E., Dornelas, M., Moyes, F. & Henderson, P. A. Temporal β diversity—A macroecological perspective. *Glob. Ecol. Biogeogr.* **28**, 1949–1960 (2019).
11. Korhonen, J. J., Soininen, J. & Hillebrand, H. A quantitative analysis of temporal turnover in aquatic species assemblages across ecosystems. *Ecology* **91**, 508–517 (2010).
12. Blowes, S. A. *et al.* The geography of biodiversity change in marine and terrestrial assemblages. *Science* **366**, 339–345 (2019).
13. Antão, L. H. *et al.* Temperature-related biodiversity change across temperate marine and terrestrial systems. *Nat. Ecol. Evol.* **4**, 927–933 (2020).
14. Pilotto, F. *et al.* Meta-analysis of multidecadal biodiversity trends in Europe. *Nat. Commun.* **11**, 3486 (2020).
15. O'Sullivan, J. D., Terry, J. C. D. & Rossberg, A. G. Intrinsic ecological dynamics drive biodiversity turnover in model metacommunities. *Nat. Commun.* **12**, 3627 (2021).
16. White, E. P. *et al.* A comparison of the species-time relationship across ecosystems and taxonomic groups. *Oikos* **112**, 185–195 (2006).
17. Rivett, D. W., Mombrikotb, S. B., Gweon, H. S., Bell, T. & van der Gast, C. Bacterial communities in larger islands have reduced temporal turnover. *ISME J.* **15**, 2947–2955 (2021).
18. Baselga, A. Partitioning the turnover and nestedness components of beta diversity. *Glob. Ecol. Biogeogr.* **19**, 134–143 (2010).
19. Tatsumi, S., Iritani, R. & Cadotte, M. W. Temporal changes in spatial variation: partitioning the extinction and colonisation components of beta diversity. *Ecol. Lett.* (2021) doi:10.1111/ele.13720.
20. Gotelli, N. J. *et al.* Long-term changes in temperate marine fish assemblages are driven by a small subset of species. *Glob. Change Biol.* **28**, 46–53 (2022).
21. Magurran, A. E. & Henderson, P. A. Explaining the excess of rare species in natural species abundance distributions. *Nature* **422**, 714–716 (2003).
22. Collins, S. L., Micheli, F. & Hartt, L. A method to determine rates and patterns of variability in ecological communities. *Oikos* **91**, 285–293 (2000).
23. Russell, G. J., Diamond, J. M., Pimm, S. L. & Reed, T. M. A Century of Turnover: Community Dynamics at Three Timescales. *J. Anim. Ecol.* **64**, 628–641 (1995).
24. Pardieck, K. L., Ziolkowski, D. J., Jr., Lutmerding, M., Aponte, V. I. & Hudson, M.-A. R. *North American Breeding Bird Survey Dataset 1966 - 2019: U.S. Geological Survey data release (https://www.pwrc.usgs.gov/BBS/RawDat*

a/. https://doi.org/10.5066/P9J6QUF6 (2020).

25. Kennedy, C. M., Oakleaf, J. R., Theobald, D. M., Baruch-Mordo, S. & Kiesecker, J. Managing the middle: A shift in conservation priorities based on the global human modification gradient. *Glob. Change Biol.* **25**, 811–826 (2019).
26. Fink, D. *et al.* eBird Status and Trends, Data Version: 2020 https://doi.org/10.2173/ebirdst.2020. *Cornell Lab Ornithol. Ithaca N. Y.* (2021).
27. Schipper, A. M. *et al.* Contrasting changes in the abundance and diversity of North American bird assemblages from 1971 to 2010. *Glob. Change Biol.* **22**, 3948–3959 (2016).
28. Jarzyna, M. A. & Jetz, W. A near half-century of temporal change in different facets of avian diversity. *Glob. Change Biol.* **23**, 2999–3011 (2017).
29. Diamond, J. M. Avifaunal equilibria and species turnover rates on the channel islands of california. *Proc. Natl. Acad. Sci.* **64**, 57–63 (1969).
30. Diamond, J. M. & May, R. M. Species Turnover Rates on Islands: Dependence on Census Interval. *Science* **197**, 266–270 (1977).
31. Nichols, J. D., Boulinier, T., Hines, J. E., Pollock, K. H. & Sauer, J. R. Estimating Rates of Local Species Extinction, Colonization, and Turnover in Animal Communities. *Ecol. Appl.* **8**, 1213–1225 (1998).
32. Ontiveros, V. J., Capitán, J. A., Casamayor, E. O. & Alonso, D. The characteristic time of ecological communities. *Ecology* **102**, e03247 (2021).
33. Kalyuzhny, M. *et al.* Niche versus neutrality: a dynamical analysis. *Am. Nat.* **184**, 439–46 (2014).
34. Rosenberg, K. V. *et al.* Decline of the North American avifauna. *Science* **366**, 120–124 (2019).
35. Di Cecco, G. J. & Hurlbert, A. H. Anthropogenic drivers of avian community turnover from local to regional scales. *Glob. Change Biol.* **28**, 770–781 (2022).
36. White, E. P. Two-phase species–time relationships in North American land birds. *Ecol. Lett.* **7**, 329–336 (2004).
37. Rittenhouse, C. D. *et al.* Land-Cover Change and Avian Diversity in the Conterminous United States. *Conserv. Biol.* **26**, 821–829 (2012).
38. Brice, M.-H., Cazelles, K., Legendre, P. & Fortin, M.-J. Disturbances amplify tree community responses to climate change in the temperate–boreal ecotone. *Glob. Ecol. Biogeogr.* **28**, 1668–1681 (2019).
39. Olden, J. D. & Rooney, T. P. On defining and quantifying biotic homogenization. *Glob. Ecol. Biogeogr.* **15**, 113–120 (2006).
40. Rossberg, A. G., Caskenette, A. L. & Bersier, L. F. Structural instability of food webs and food-web models and their implications for management. in *Adaptive Food Webs: Stability and Transitions of Real and Model Ecosystems* (eds. Moore, J. C., de Ruiter, P. C., McCann, K. S. & Wolters, V.) 372–383 (Cambridge University Press, 2017). doi:10.1017/9781316871867.024.
41. Martin, P. R. & Bonier, F. Species interactions limit the occurrence of urban-adapted birds in cities. *Proc. Natl. Acad. Sci.* **115**, E11495–E11504 (2018).
42. Freeman, B. G., Strimas-Mackey, M. & Miller, E. T. Interspecific competition limits bird species' ranges in tropical mountains. *Science* **377**, 416–420 (2022).
43. Rossberg, A. G. *Food Webs and Biodiversity: Foundations, Models, Data*. (John Wiley & Sons, Ltd, 2013).
44. Blanchet, F. G., Cazelles, K. & Gravel, D. Co-occurrence is not evidence of ecological interactions. *Ecol. Lett.* **23**, 1050–1063 (2020).
45. O'Sullivan, J. D., Knell, R. J. & Rossberg, A. G. Metacommunity-scale biodiversity regulation and the self-organised emergence of macroecological patterns. *Ecol. Lett.* **22**, 1428–1438 (2019).
46. Zhang, W., Sheldon, B. C., Grenyer, R. & Gaston, K. J. Habitat change and biased sampling influence estimation of diversity trends. *Curr. Biol.* **31**, 3656-3662.e3 (2021).

47. Farwell, L. S., Elsen, P. R., Razenkova, E., Pidgeon, A. M. & Radeloff, V. C. Habitat heterogeneity captured by 30-m resolution satellite image texture predicts bird richness across the United States. *Ecol. Appl.* **30**, e02157 (2020).
48. Hurlbert, A. H. & White, E. P. Disparity between range map- and survey-based analyses of species richness: patterns, processes and implications. *Ecol. Lett.* **8**, 319–327 (2005).
49. Boulinier, T., Nichols, J. D., Sauer, J. R., Hines, J. E. & Pollock, K. H. Estimating Species Richness: The Importance of Heterogeneity in Species Detectability. *Ecology* **79**, 1018–1028 (1998).
50. Jarzyna, M. A. & Jetz, W. Detecting the Multiple Facets of Biodiversity. *Trends Ecol. Evol.* **31**, 527–538 (2016).
51. Doak, D. F. & Morris, W. F. Demographic compensation and tipping points in climate-induced range shifts. *Nature* **467**, 959–962 (2010).
52. Nolan, C. *et al.* Past and future global transformation of terrestrial ecosystems under climate change. *Science* **361**, 920–923 (2018).
53. Sauer, J. R. *et al.* The first 50 years of the North American Breeding Bird Survey. *The Condor* **119**, 576–593 (2017).
54. Dorazio, R. M. & Royle, J. A. Estimating Size and Composition of Biological Communities by Modeling the Occurrence of Species. *J. Am. Stat. Assoc.* **100**, 389–398 (2005).
55. Sauer, J. R., Fallon, J. E. & Johnson, R. Use of North American Breeding Bird Survey Data to Estimate Population Change for Bird Conservation Regions. *J. Wildl. Manag.* **67**, 372–389 (2003).
56. Shimadzu, H., Dornelas, M. & Magurran, A. E. Measuring temporal turnover in ecological communities. *Methods Ecol. Evol.* **6**, 1384–1394 (2015).
57. Legendre, P. A temporal beta-diversity index to identify sites that have changed in exceptional ways in space–time surveys. *Ecol. Evol.* **9**, 3500–3514 (2019).
58. Leung, B. *et al.* Clustered versus catastrophic global vertebrate declines. *Nature* **588**, 267–271 (2020).
59. Fink, D. *et al.* Modeling avian full annual cycle distribution and population trends with citizen science data. *Ecol. Appl.* **30**, e02056 (2020).
60. Santini, L. *et al.* Assessing the suitability of diversity metrics to detect biodiversity change. *Biol. Conserv.* **213**, 341–350 (2017).
61. Carpenter, B. *et al.* Stan: A Probabilistic Programming Language. *J. Stat. Softw.* **76**, (2017).
62. Bürkner, P.-C. Advanced Bayesian Multilevel Modeling with the R Package brms. *R J.* **10**, 395–411 (2018).
63. Carey, S., Ostling, A., Harte, J. & del Moral, R. Impact of Curve Construction and Community Dynamics on the Species–Time Relationship. *Ecology* **88**, 2145–2153 (2007).

Extended Data

SI 1

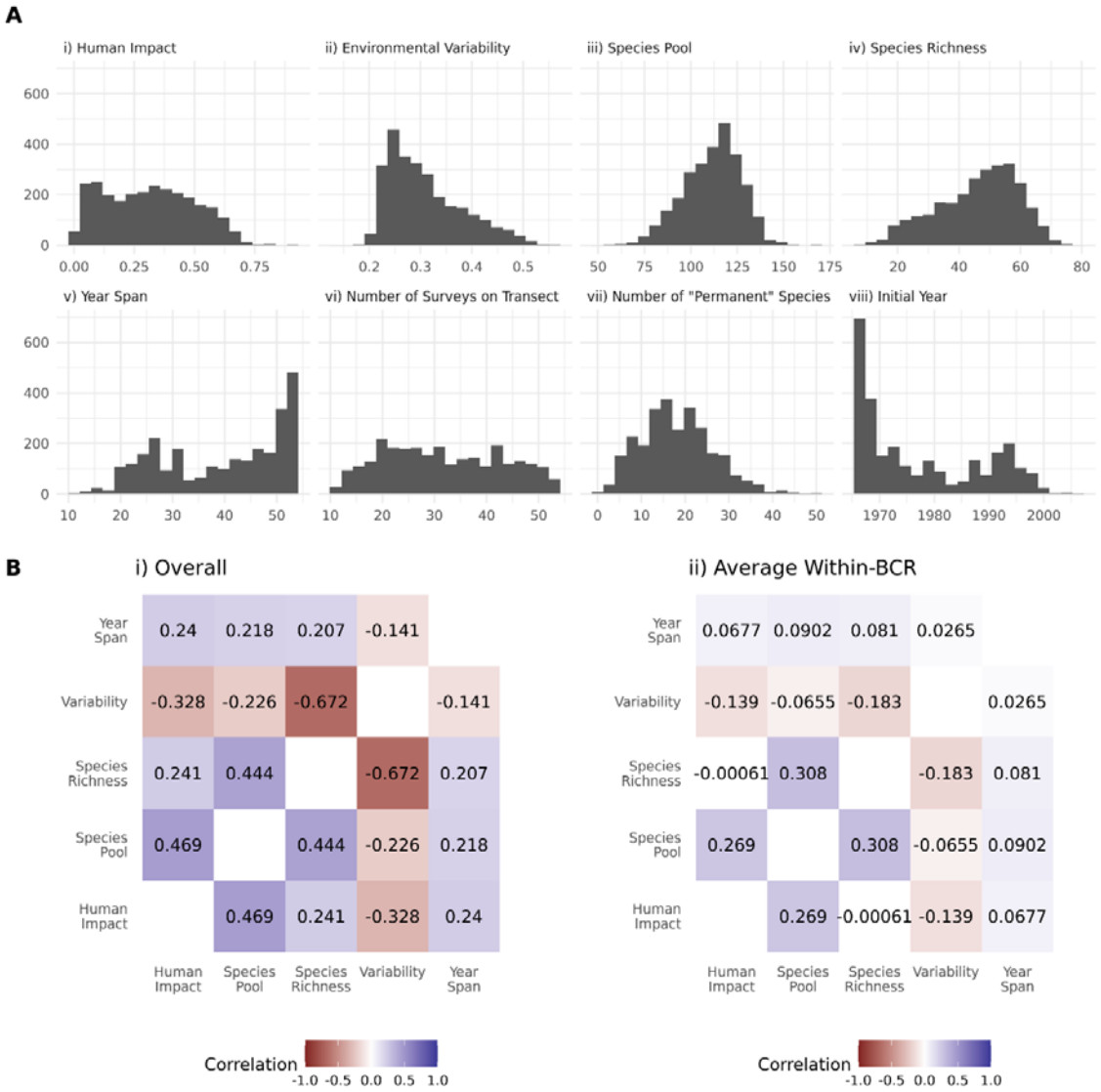

SI 1 Predictor variable data summaries. A) Distribution of key predictors and summary statistics. Histograms are shown across all transects and values are shown before scaling used in regressions. Permanent species (g) are operationally defined as those seen in every year the transect survey was included. B) Correlation between key predictor variables i) across all transects ii) within each BCR, then averaged.

SI 2

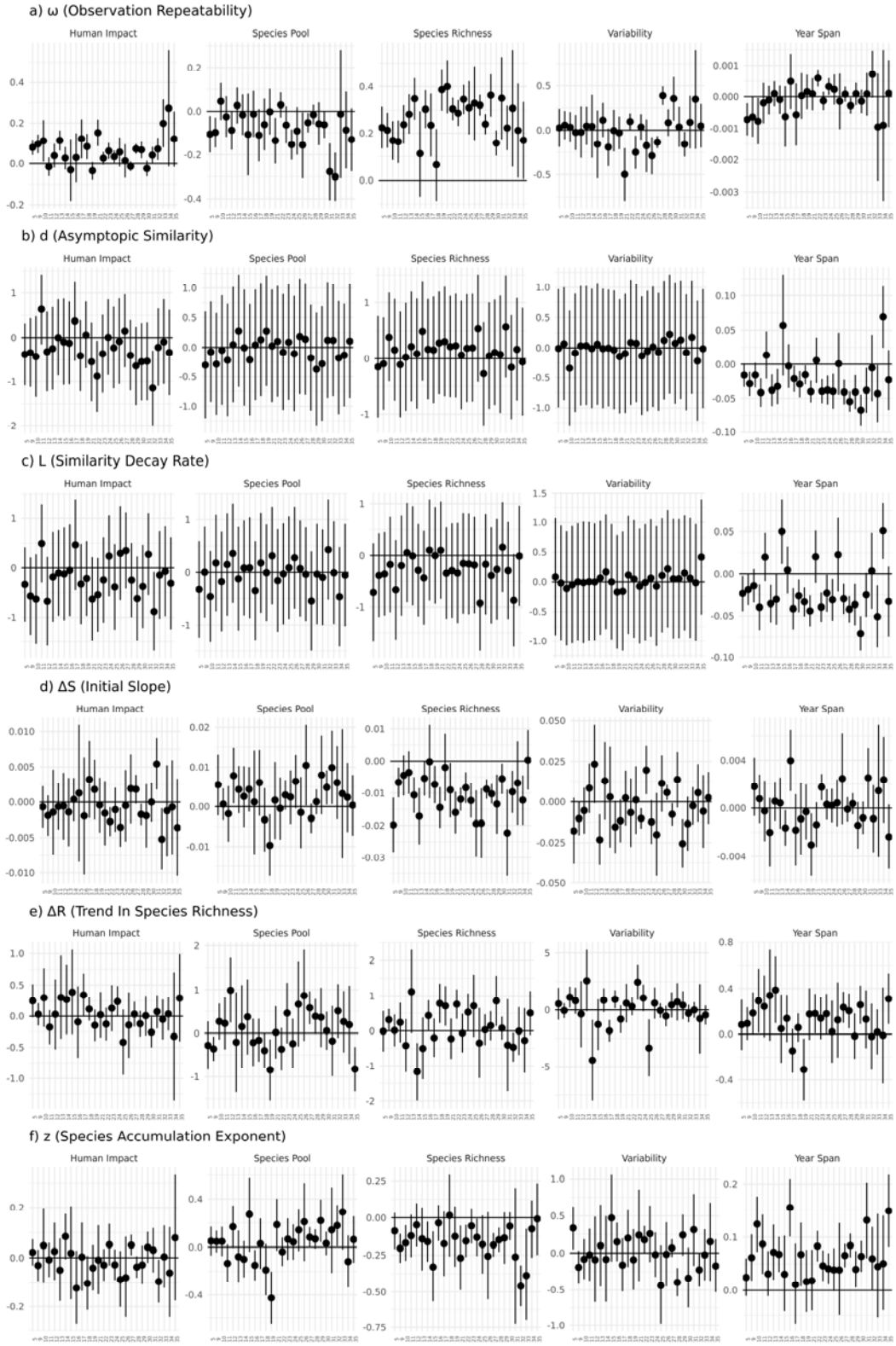

SI 2 Fitted coefficients for each predictor for each Bird Conservation Region (BCR). Each BCR is given by its number (see Fig 2 for description). Points show the mean estimate, while error bars show two standard errors around each mean estimate.

SI 3

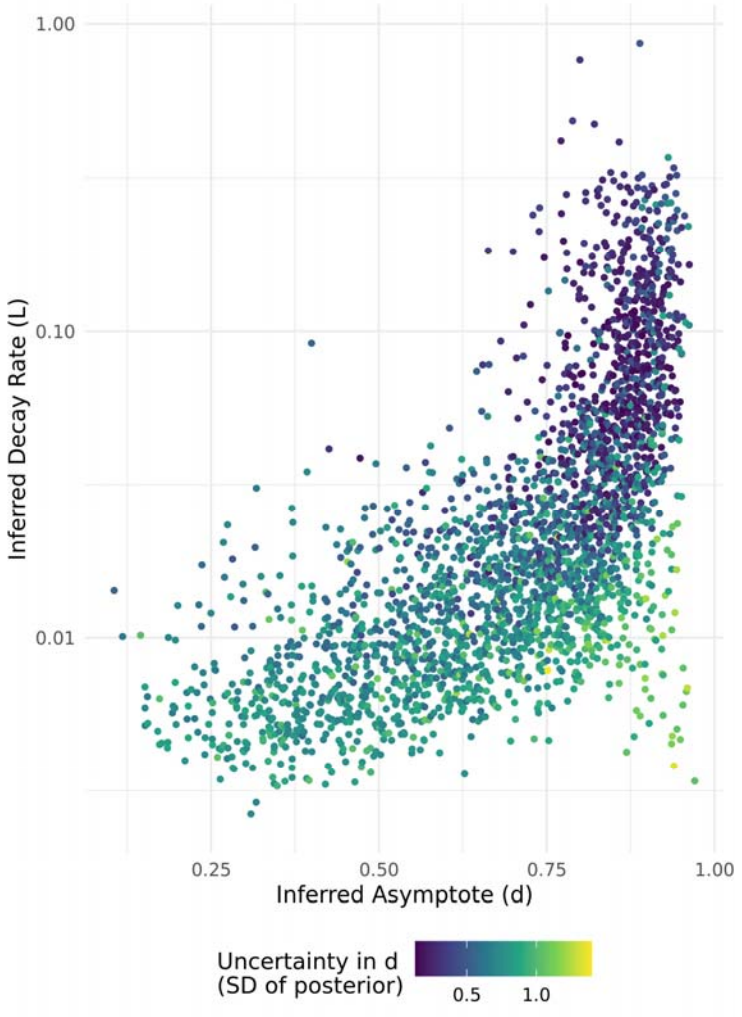

SI 3. Correlation in estimated curve parameters. Posterior means of similarity decay curve parameters when directly fitted i.e. without the predictor variables. Results are shown across all Bird Conservation Regions. Points are coloured by the uncertainty in the asymptote (standard deviation of the posterior on the logit scale). There is a clear positive correlation between the d and L parameters from which we can broadly identify three archetypes of observable temporal similarity dynamics. At the top right, 'fast' transects with high L and high d, show a quick decline to a clear high asymptote. At the bottom right, 'slow' transects with low L and low d show a clear saturation, but take considerably longer to reach that point. Thirdly, in the bottom right there are a smaller group of 'uncertain' transects where the asymptote is uncertain. These are frequently transects with shorter available time series (Year Span).

SI 4

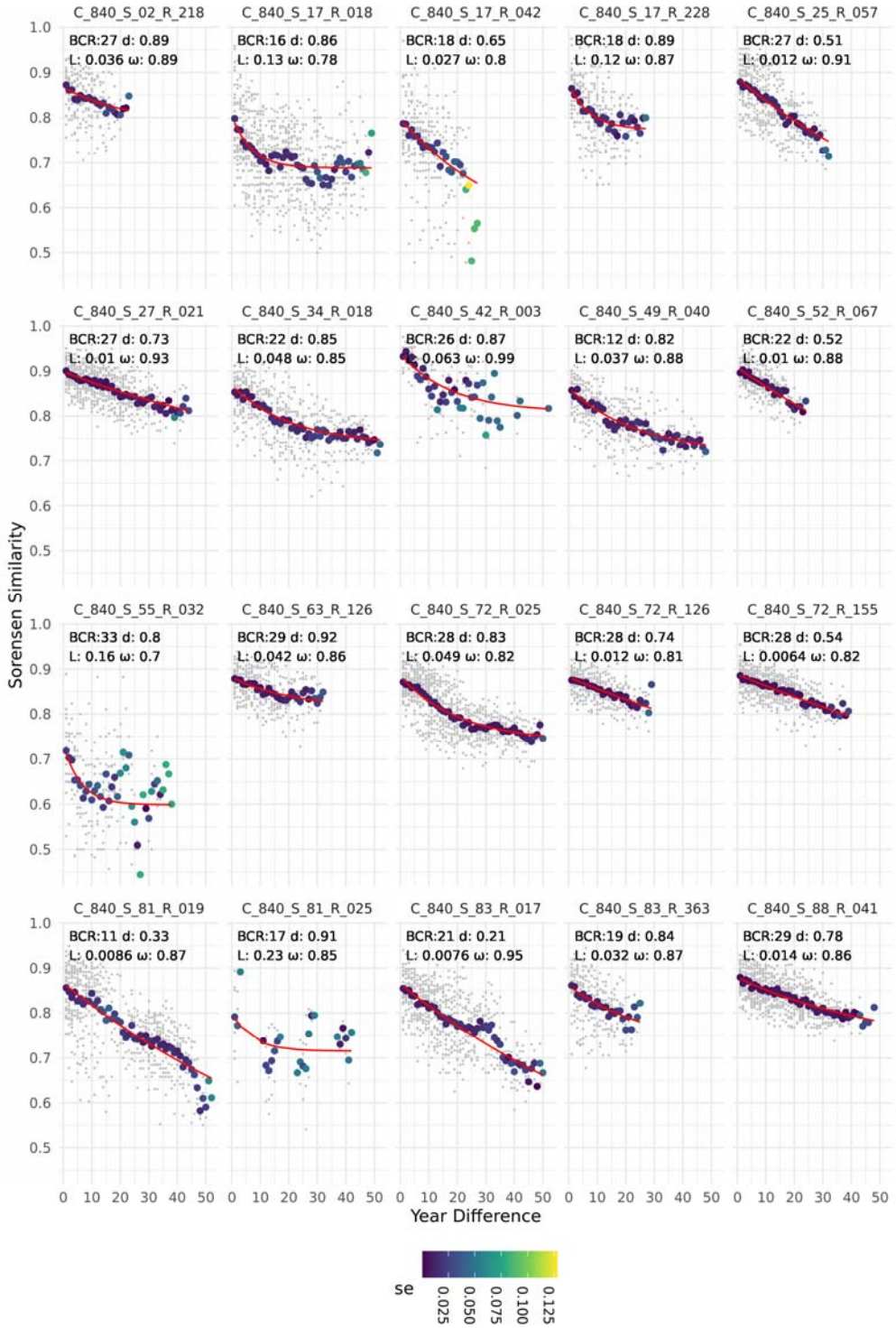

SI 4. Randomly selected examples of similarity-decay curves. Colour of each point shows the confidence assigned to each estimate of the mean similarity for that year difference, calculated as a standard error. Small grey dots are each similarity value underlying these averages. Red line shows the directly fit (i.e without the predictor variables, but with the partial pooling) decay curve using the mean of the posterior values. Transects are titled by country code (US = 840), state code and route number. Curve parameters and BCR number are shown for each transect.

SI 5

Details of hierarchical model used for fitting similarity decay curve. The model is described in the main text methods, but here we give further specific details. Each BCR was fit separately in *brms* 2.18, an R package that calls STAN. All code (including the generated STAN code) is available online, as well as the fitted model objects. The central *brms* call was:

```
Model<- brm( data =  Data_filt_CENTERED,
             bf(y|se(se, sigma =TRUE)~ (om0+betaoHM*C_HM + betaoCV*C_CV + betaoAL*C_AL + betaoGM*C_GM + betaoYS*C_YS)*(
               (1-inv_logit(logitd0 +betadHM*C_HM + betadCV*C_CV + betadAL*C_AL + betadGM*C_GM + betadYS*C_YS)) *
                 exp(-exp(logL0+betaLHM*C_HM + betaLCV*C_CV + betaLAL*C_AL + betaLGM*C_GM + betaLYS*C_YS )*x)+
                 inv_logit(logitd0 +betadHM*C_HM + betadCV*C_CV + betadAL*C_AL + betadGM*C_GM + betadYS*C_YS)),
               om0+logitd0+logL0  ~ 1+ (1|TransectID),
               betaoHM+betaoCV+betaoAL+betaoGM + betaoYS ~1,
               betaLHM+betaLCV+betaLAL+betaLGM + betadYS ~1,
               betadHM+betadCV+betadAL+betadGM + betaLYS ~1,
               sigma   ~ 1 +(1|TransectID),
               nl = TRUE),
             iter = 10000, thin =5,

             prior = prior(normal(0.8, 1), lb=0, ub = 1, nlpar = "om0") +
               prior(normal(-2.3, 1), lb=-4,ub = -1, nlpar = "logL0")+
               prior(normal(logit(0.5), 1), nlpar = "logitd0")+
               prior(normal(0, 0.5),nlpar = "betadHM") +
               prior(normal(0, 0.5),nlpar = "betadCV") +
               prior(normal(0, 0.5),nlpar = "betadAL") +
               prior(normal(0, 0.5),nlpar = "betadGM") +
               prior(normal(0, 0.5),nlpar = "betadYS") +
               prior(normal(0, 0.5),nlpar = "betaoHM") +
               prior(normal(0, 0.5),nlpar = "betaoCV") +
               prior(normal(0, 0.5),nlpar = "betaoAL") +
               prior(normal(0, 0.5),nlpar = "betaoGM") +
               prior(normal(0, 0.5),nlpar = "betaoYS") +
               prior(normal(0, 0.5),nlpar = "betaLHM") +
               prior(normal(0, 0.5),nlpar = "betaLCV") +
               prior(normal(0, 0.5),nlpar = "betaLAL") +
               prior(normal(0, 0.5),nlpar = "betaLGM") +
               prior(normal(0, 0.5),nlpar = "betaLYS") +
               prior(normal(0,1), class = "sd", group = "TransectID", nlpar = "om0")+
               prior(normal(0,0.1), class = "sd", group = "TransectID", nlpar = "logL0")+
               prior(normal(0,0.5), class = "sd", group = "TransectID", nlpar ="logitd0"),
             cores = 4)
```

where the input data is separate for each BCR and has columns:

- x = Difference in years between samples
- y= Average Sorensen similarity
- se = Standard error of the estimate of y.
- TransectID = character string identifying the transect
- C_HM = Human modification Index value of transect (centred)
- C_CV = Environmental Variability value of transect (centred)
- C_AL = Observed Species Richness value of transect(centred)
- C_GM = Species Pool value of transect (centred)
- C_YS = Year Span value of transect (centred)

The full model to determine the likelihood (excluding the priors) of each average Sorensen similarity $\overline{S_{t,1}}$ with time-difference t on transect i is:

$$\mathcal{L} \sim \mathcal{N}\left(\overline{S_{t,1}} - \overline{S_{t,1}}_{obs}\,, \qquad \sigma_0 + \epsilon_i^{\sigma}\right)$$

where

$$\overline{S_{t,1}} \;=\; \omega_i[(1-d_i)e^{-L_i t} + d_i]$$

and:

$$\mathrm{logit}(d_i) = d_0 + \epsilon_i^d + \beta_{HM}^d C_{HM_i} + \beta_{CV}^d C_{CV_i} + \beta_{AL}^d C_{AL_i} + \beta_{GM}^d C_{GM_i} + \beta_{YS}^d C_{YS_i} + \epsilon^{\mathrm{d}}$$

$$log(L_i) = L_0 + \epsilon_i^L + \beta_{HM}^L C_{HM_i} + \beta_{CV}^L C_{CV_i} + \beta_{AL}^L C_{AL_i} + \beta_{GM}^L C_{GM_i} + \beta_{YS}^L C_{YS_i} + \epsilon^{\mathrm{L}}$$

$$\omega_i = \omega_0 + \epsilon_i^{\omega} + \beta_{HM}^{\omega} C_{HM_i} + \beta_{CV}^{\omega} C_{CV_i} + \beta_{AL}^{\omega} C_{AL_i} + \beta_{GM}^{\omega} C_{GM_i} + \beta_{YS}^{\omega} C_{YS_i} + \epsilon^{\omega}$$

with the hierarchical pooling terms to specify different intercepts for term for each transect i are defined based on Normal distributions, each with a fitted standard deviation:

$$\epsilon_i^d \sim \mathcal{N}(0, d_\sigma)$$
$$\epsilon_i^L \sim \mathcal{N}(0, L_\sigma)$$
$$\epsilon_i^\omega \sim \mathcal{N}(0, \omega_\sigma)$$
$$\epsilon_i^\sigma \sim \mathcal{N}(0, \sigma_\sigma)$$

Priors not manually specified above follow the weak defaults of brms. The complete list of priors were:

		Distribution	Parameters	Bounds		Notes
				Lower	Upper	
Regression intercept terms						
	d_0	Normal	Mean =0, sd =1			NB logit term
	L_0	Normal	Mean = -2.3, sd = 1	-4	-1	NB log term
	ω_0	Normal	Mean = 0.8, sd = 1	0	1	
Regression Main Effect Terms						
	All β	Normal	Mean = 0, sd = 0.5			
Regression Error Terms						
	ϵ^d	Student t	Df = 3, loc = 0, scale = 2.5	0		
	ϵ^L	Student t	Df = 3, loc = 0, scale = 2.5	0		
	ϵ^ω	Student t	Df = 3, loc = 0, scale = 2.5	0		
Partial pooling across transects						
	d_σ		Mean = 0, sd = 0.5	0		Prior on difference between transects
	L_σ		Mean = 0, sd = 0.1	0		
	ω_σ		Mean = 0, sd = 1	0		
Overall Error						
	σ_0	Student t	Df = 3, loc = 0, scale = 2.5			Average error between estimate and observation
	σ_σ	Student t	Df = 3, loc = 0, scale = 2.5	0		Difference between extent of error between transects